Video Article

Rose Bengal Photothrombosis by Confocal Optical Imaging *In Vivo*: A Model of Single Vessel Stroke

Lora Talley Watts[1], Wei Zheng[1], R. Justin Garling[2], Victoria C. Frohlich[3], James Donald Lechleiter[1]

[1]Department of Cellular and Structural Biology, The University of Texas Health Science Center San Antonio

[2]School of Medicine, The University of Texas Health Science Center San Antonio

[3]Cell & Tissue Imaging Center, St. Jude Children#s Research Hospital

Correspondence to: James Donald Lechleiter at lechleiter@uthscsa.edu

Abstract

In vivo imaging techniques have increased in utilization due to recent advances in imaging dyes and optical technologies, allowing for the ability to image cellular events in an intact animal. Additionally, the ability to induce physiological disease states such as stroke *in vivo* increases its utility. The technique described herein allows for physiological assessment of cellular responses within the CNS following a stroke and can be adapted for other pathological conditions being studied. The technique presented uses laser excitation of the photosensitive dye Rose Bengal *in vivo* to induce a focal ischemic event in a single blood vessel.

The video protocol demonstrates the preparation of a thin-skulled cranial window over the somatosensory cortex in a mouse for the induction of a Rose Bengal photothrombotic event keeping injury to the underlying dura matter and brain at a minimum. Surgical preparation is initially performed under a dissecting microscope with a custom-made surgical/imaging platform, which is then transferred to a confocal microscope equipped with an inverted objective adaptor. Representative images acquired utilizing this protocol are presented as well as time-lapse sequences of stroke induction. This technique is powerful in that the same area can be imaged repeatedly on subsequent days facilitating longitudinal *in vivo* studies of pathological processes following stroke.

Video Link

The video component of this article can be found at https://www.jove.com/video/52794/

Introduction

The technique described permits visualization of *in vivo* cellular responses immediately following induction of Rose Bengal photothrombosis in an intact mouse. Rose Bengal (4,5,6,7-tetrachloro-2',4',5',7'-tetraiodofluorescein) is a photosensitive dye used to induce ischemic stroke in animal models (mouse and rat). Following a bolus injection of RB through the tail vein and subsequent illumination through a thinned skull with a 564 nm laser light, a thrombus is induced causing a physiologic stroke[1]. The method was originally described by Rosenblum and El-Sabban in 1977, and was later adapted by Watson in the mid 1980s[1,2]. In brief, Rose Bengal is irradiated with green excitation light (561 nm laser in our case), which generates the production of reactive oxygen species, which subsequently activates tissue factor, an initiator of the coagulation cascade. The induction of the coagulation cascade produces an ischemic lesion that is pathologically relevant to clinical stroke[3].

Stroke has a complex pathophysiology due to the interplay of many different cells types including neurons, glia, endothelium and the immune system. Choosing the best technique to study a particular cellular process requires multiple considerations. Experimental techniques fall broadly into one of three categories: *in vitro*, *in vivo* and *in silico* with each having advantages and disadvantages. *In vitro* studies have the primary disadvantage of removing cells from their natural environment and therefore may not reproduce effects seen in an intact, living animal. *In vivo* techniques provide for enhanced experimental replication of disease states with increased translational significance. *In silico* generally refers to computer modeling of a disease or cellular process, and while increasingly utilized to study potential drug interactions for example, any information gleaned must still be tested in living cells or tissue.

The ideal model of stroke in the laboratory setting should demonstrate similar pathological features to those seen in the human population. While there are common physiologic characteristics of stroke in the human population, there are also many differences depending on the type of injury experienced. Stroke in the human population occurs as small or large vessel occlusions, hemorrhagic lesions, and artery-to artery or cardio-embolisms that result in varied infarct volumes as well as differences in mechanisms related to each pathology. The advantage of utilizing animal stroke models is the generation of reproducible infarcts that mimic characteristics of human stroke. The most common animal stroke models include artery occlusion using: middle cerebral artery occlusion (embolic or endovascular filament methods) which models distal MCAO and the photothrombosis model. The advantages and disadvantages of each model have been reviewed elsewhere (see [4] and [5]). Global ischemic models (MCAO), while relatively easy to perform are less relevant to human stroke than are focal stroke models. In addition, these methods are highly variable in inducing reproducible brain infarct lesions. The photothrombosis model is highly reproducible as long as the experimenter

controls their experiments well, providing a clear advantage over MCAO models. However, due to microvasculature insult the model has been described to display a minimal ischemic penumbra, the area where cells are thought to be salvageable [6,7]. Additionally, vasogenic edema and cytotoxic edema formation may also be induced following irradiation of the imaging area. Despite these limitations the technique has provided new insight into many physiological processes following stroke[8,9,10,11].

Protocol

Note: All animal procedures were approved by the Institutional Animal Care and Use Committee of the University of Texas Health Science Center San Antonio and were consistent with the ARRIVE guidelines.

1. Anesthetizing for Cortical Preparation

1. Place the mouse in an induction chamber with 2-3% isofluorane mixed with oxygen to induce anesthesia. Observe the respiration rate decrease as the mouse is induced. Pinch the paw of the mouse to determine whether the mouse is ready to move to the nose cone. Note: Anesthesia level is a critical step in any *in vivo* preparation and care should be taken not to induce a level that will cause global ischemia.
2. Once the mouse is sufficiently anesthetized, transfer the animal to the surgery/imaging platform and place the mouse's nose in the nose cone and apply 1-1.2% isofluorane to maintain an anesthetized state. Ensure that the mouse is lying on a temperature controlled heating pad to maintain the body temperature (37°C +/- 0.5°C) throughout the remaining procedures. Place vet ointment over the eyes to prevent dryness while under anesthesia.
3. Monitor the physiology of the mouse using a pulse oximetry system using the tail or foot clip provided with the system. Check that the respiratory rate is maintained between 50-65 breaths/min. Check that the heart rate remains between 300 to 450 bpm and oxygen saturation is maintained between 97-98% to ensure long-term survival of the animal.
4. When the mouse is adequately anesthetized, shave the hair over the cranium using electric clippers, remove residual hair and clean with betadine, followed by an ethanol swab. Repeat this procedure up to three times to ensure a sterile surgical environment.

2. Surgical Procedure

1. With the scalp fully cleaned and shaven, make a 5 mm incision in the scalp of the mouse to reveal the cranial fissures and to locate bregma.
2. Use a sterile cotton applicator to remove any remaining fascia overlying the cranium.
3. Glue a custom made stainless steel ring (**Figure 1**) with tissue adhesive to the bone overlying the parietal cortex using the stereotaxic coordinates of Bregma: -1 to -3 mm and lateral: 2-4 mm. Note: The glue typically sets within 2 min after the placement of the ring onto the bone.
4. Affix the ring to a stereotaxic holder (**Figure 2**) to stabilize the mouse and to prevent movement during imaging.
5. Under a surgical grade dissecting microscope, slowly drill a 1-2 mm section in the cranium using a speed controlled dremel-like tool (Meisinger 3.9 mm drill bit) making sure to keep the area level as it is drilled. Achieve this using a zig-zag pattern. To avoid heat build up, set the drill speed to low and take frequent breaks.
6. When the cranial skull becomes shinny in appearance, continue the thinning of the skull using a scalpel blade utilizing the same zig-zag pattern to keep the thinned surface level to facilitate smooth removal of thin layers of cranial skull. Using the tip of the scalpel blade make small linear strokes with light pressure to remove thin layers of bone at a time. Continue this until the vasculature is clearly visible through the dissecting microscope.
7. If the experimenter punctures through or break the skull during the thinning process, euthanize the animal due to likely damage to the underlying cortex.
   Note: The mouse skull is approximately 300 µm in thickness and is comprised of two thin layers of compact bone (one external and one internal layer) and a layer of spongy bone sandwiched between the two layers of compact bone. The external layer of compact bone and most of the spongy bone are removed within the 5 mm drilling area resulting in an approximate 50 µm layer of compact bone remaining (see **Figure 2B**). Visualization of the vasculature will ensure that the final intact thinned skull is approximately 50 µm in thickness. The skull is therefore still present when thinned to this thickness.

3. Microscope Set-up

1. Use an inverted microscope system (conventional, confocal or two-photon systems) that has an objective inverter. Note: It is also possible to utilize a standard upright microscope. The limiting factor will be the space between the stage and the objectives. Modifications to the stage may be necessary to accomplish this setup.
2. Secure the surgical/imaging platform to a custom made stage that is located aside the base of the microscope. Note: The platform is made using a laboratory jack to allow vertical movement of the surgical/imaging platform under the objective. The laboratory jack is mounted to a plate affixed to four cylindrical poles. (See **Figure 2**).
3. Position the objective inverter containing a 20X objective over the cranial window. Use an external light source to find the cranial window by looking through the eyepieces of the microscope and position the objective in the imaging area. Note: The imaging area will be denoted by the presence of the vasculature.
4. For water-based objectives, use artificial cerebral spinal fluid (aCSF) (130 mM NaCl; 30 mM KCl; 12 mM KH_2PO_4; 200 mM $NaHCO_3$; 30 mM HEPES; and 100 mM glucose) as the medium due to potential leakage into the cranial cavity during imaging (**Figure 3**).

4. Rose Bengal Dye Preparation, Administration and Induction of Stroke

1. Prepare a fresh 20 mg/ml solution of Rose Bengal in artificial cerebral spinal fluid (aCSF); filter and sterilize before administration. Do not reuse or store the Rose Bengal once it has been mixed. Make a fresh solution for each experiment.

2. Give a 0.1 ml tail vein injection of Rose Bengal while scanning the cranial window with a 561 nm laser to ensure adequate injection of the solution. Note: Rose Bengal will be visualized within 5 sec after injection in the vasculature of the brain. The entire vessel should be filled with Rose Bengal.

3. Following adequate injection of Rose Bengal dye choose an appropriate vessel for thrombosis based on vessel diameter (40-80 μm) to ensure reproducibility of a particular lesion volume. Differentiate between arteries and veins by looking at the direction of blood flow: arteries will move from larger diameter to smaller diameter vessels, veins move from smaller to larger diameter vessels. This is easily accomplished by visualization once Rose Bengal is injected.

4. Change the microscope setting as follows:
    1. Increase the dwell time. Note: This will vary depending on the microscope system being utilized.
    2. Increase the laser power to 100%.
    3. Collect time sequence images at 1 frame/sec using the maximum scan speed.

5. Scan the mouse until a stable clot is formed within the vessel. Note: This typically is achieved within 5 min of continuous scanning (See **Figure 4**).

6. Following the induction of clot formation using Rose Bengal, remove the mouse from the imaging area back to the dissecting microscope. Carefully remove the stainless steel ring from the cranial skull. Examine the cranial window for any bleeding. If bleeding occurs, terminate the experiment.

7. Use 6.0 monofilament suture to close the incision over the skull. Place antibiotic ointment along the suture line to prevent infection. Inject Buprenex (0.05 mg/kg) subcutaneously every 12 hr for three days for pain management.

8. Return the mouse to a recovery chamber following removal from the anesthetic until fully awake and freely moving.

9. Return the mouse to a clean cage for further investigation at a later time.

5. Longitudinal Imaging on Subsequent Days

1. Employ the following methods to perform longitudinal imaging on subsequent days post-photothrombosis.
    1. Anesthetize the mouse as described in Section 1 of the methods.
    2. Upon adequate anesthesia re-open the scalp by removing any residual sutures to reopen the skin overlying the previously drilled imaging field.
    3. Use a sterile cotton applicator to remove any remaining fascia overlying the cranium.
    4. Glue a custom made stainless steel ring (**Figure 1**) with tissue adhesive to the bone overlying the previous imaging field.
    5. Affix the ring to a stereotaxic holder (**Figure 2**) to stabilize the mouse and to prevent movement during imaging.
    6. Locate the vasculature underlying the previously thinned skull. Use tail vein injection of FITC-Dextran to verify the presence of the previously induced clot.
    7. Use 6.0 monofilament suture to close the incision over the skull. Place antibiotic ointment along the suture line to prevent infection. Inject Buprenex (0.05mg/kg) subcutaneously every 12 hr for three days for pain management.
    8. Return the mouse to a recovery chamber following removal from the anesthetic until fully awake and freely moving.

6. Verification of Stroke Induction (Post-mortem)

1. At the conclusion of a study, verify stroke volume using 2,3,5-triphenyltetrazolium chloride (TTC) staining as shown in **Figure 5**. The full method can be found in[12].

Representative Results

The aim of this method was to induce an ischemic stroke in animal models (mouse and rat) following a bolus injection of RB through the tail vein and subsequent illumination of a thinned skull with a 561 nm laser light. The images in **Figure 4** demonstrate the progression of clot formation within a single vessel following irradiation of the area at 0, 1, 1.5 and 2 min. Prior to clot formation the entire vessel is white due to free flowing Rose Bengal. Following the induction of irradiation of the vessel there is an obvious darkening in portions of the vessel and indicates the induction of clot formation (frames 1 and 1.5 min). Following complete occlusion there is a marked accumulation of Rose Bengal dye (white area) preceding the clot (black area) within the vessel. The 2 minute frame demonstrates the complete occlusion of the artery.

To verify the presence of an ischemic stroke TTC staining can be utilized. TTC is a commonly used stain for the detection of cerebral infarction by the formation of red formazan TTC products in healthy tissue. The lack of formazan production (white tissue) indicates the infarct area. The areas indicated by the boxes in **Figure 5** demonstrate the typical lesion sizes obtained 1 and 5 days from two separate animals following a clot produced within a vessel approximately 80mm in diameter. Image analysis is performed on a flat bed scanner and the use of ImageJ software. Regions of interest can be drawn within ImageJ to measure the area of the stroke volume for each brain.
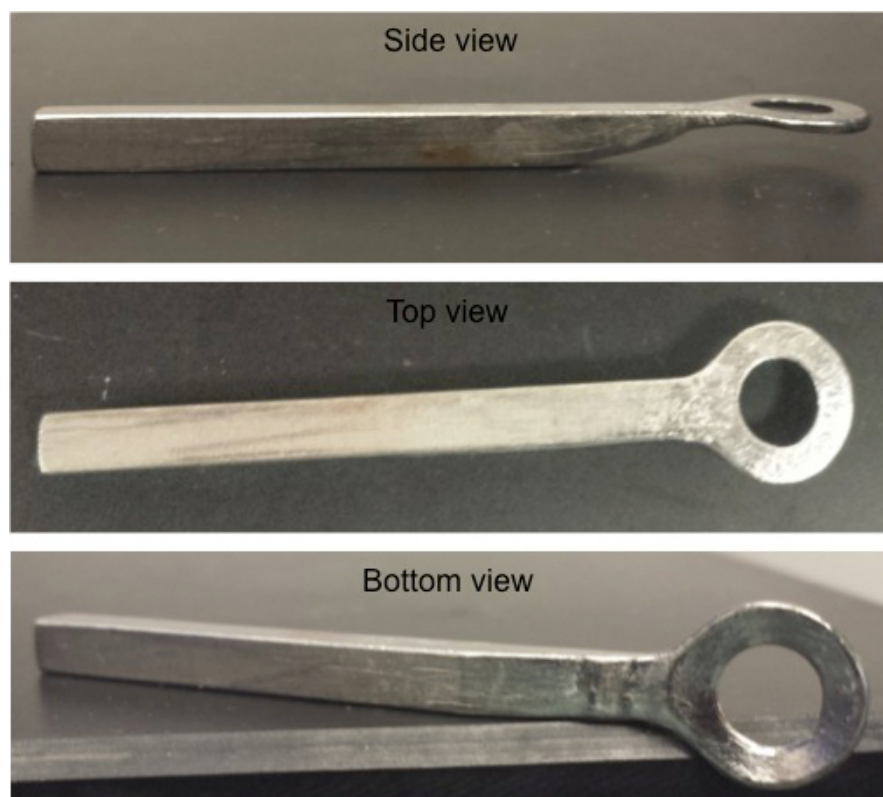
Figure 1: Stainless Steel Ring. Three views (top, side and bottom views) are shown of the stainless steel ring holder that is applied to the skull of the mouse to affix it to the stereotaxic holder.
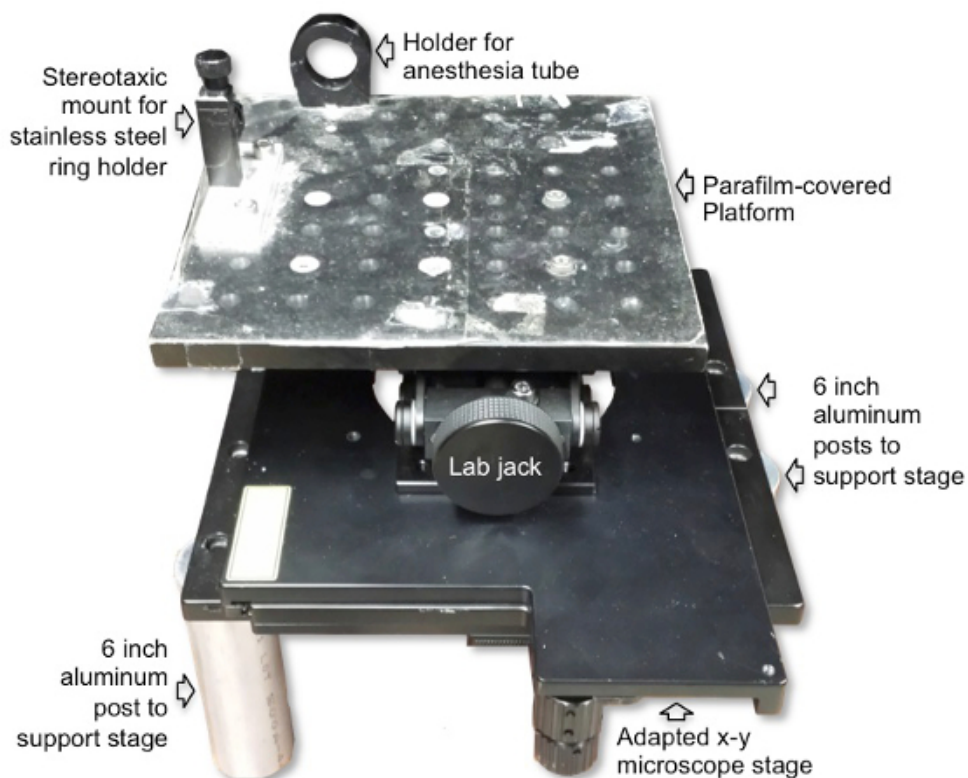
Figure 2: Microscope imaging platform setup for RB photothrombosis. The surgical/imaging platform contains a holder for the anesthesia tube with nosecone and a stereotaxic holder for the stainless steel ring that is affixed to the skull of the animal to decrease movement of the animal during imaging. The platform is placed on top of and secured to the laboratory jack to allow vertical movement for positioning the mouse under the microscope objective. The laboratory jack is then attached to a microscope stage, which allows for horizontal movement. The microscope stage is placed on top of and secured to four cylindrical poles.
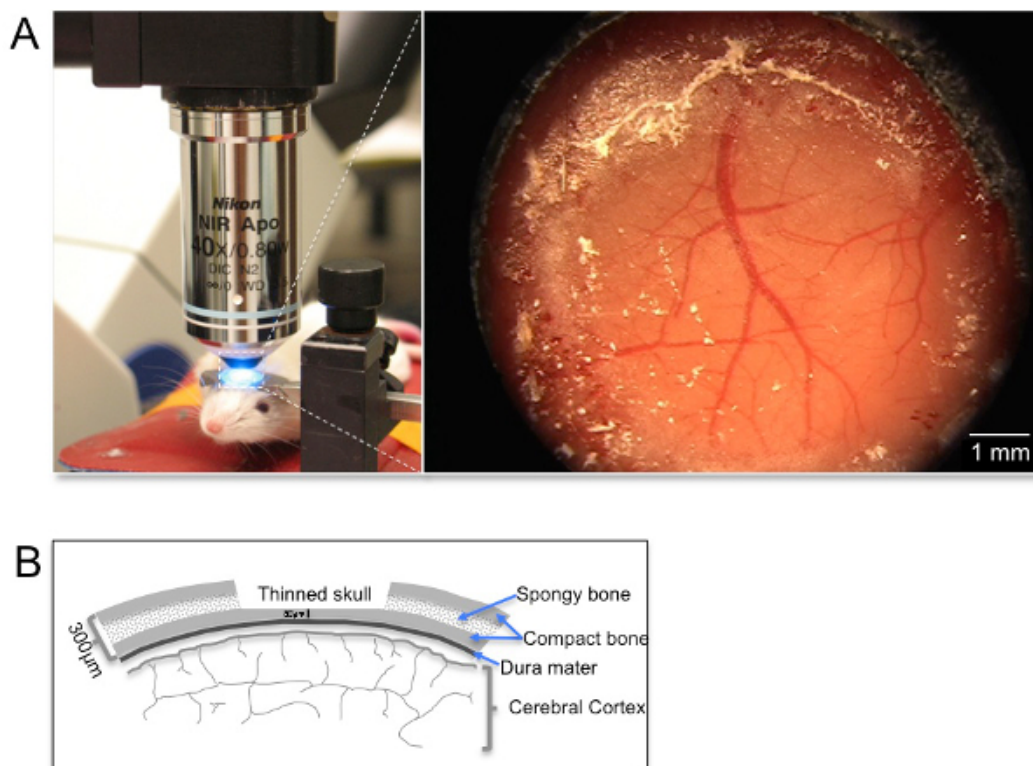
Figure 3: Picture of imaging/surgical platform design and orientation under the objective inverter. (**A**) The panel on the left demonstrates a representative image of the positioning of an anesthetized mouse (anesthesia nose cone was removed briefly for taking the picture). Note the use of a custom steel ring to attach the mouse skull to decrease the contribution of breathing artifacts throughout the imaging procedures. The image on the right demonstrates an image of the cortical window under a dissecting microscope. (**B**) Sketch of the thin skull preparation from a coronal view demonstrating the layers of the skull in relation to the dura mater and the thickness of the thinned area in relation to the full skull thickness.
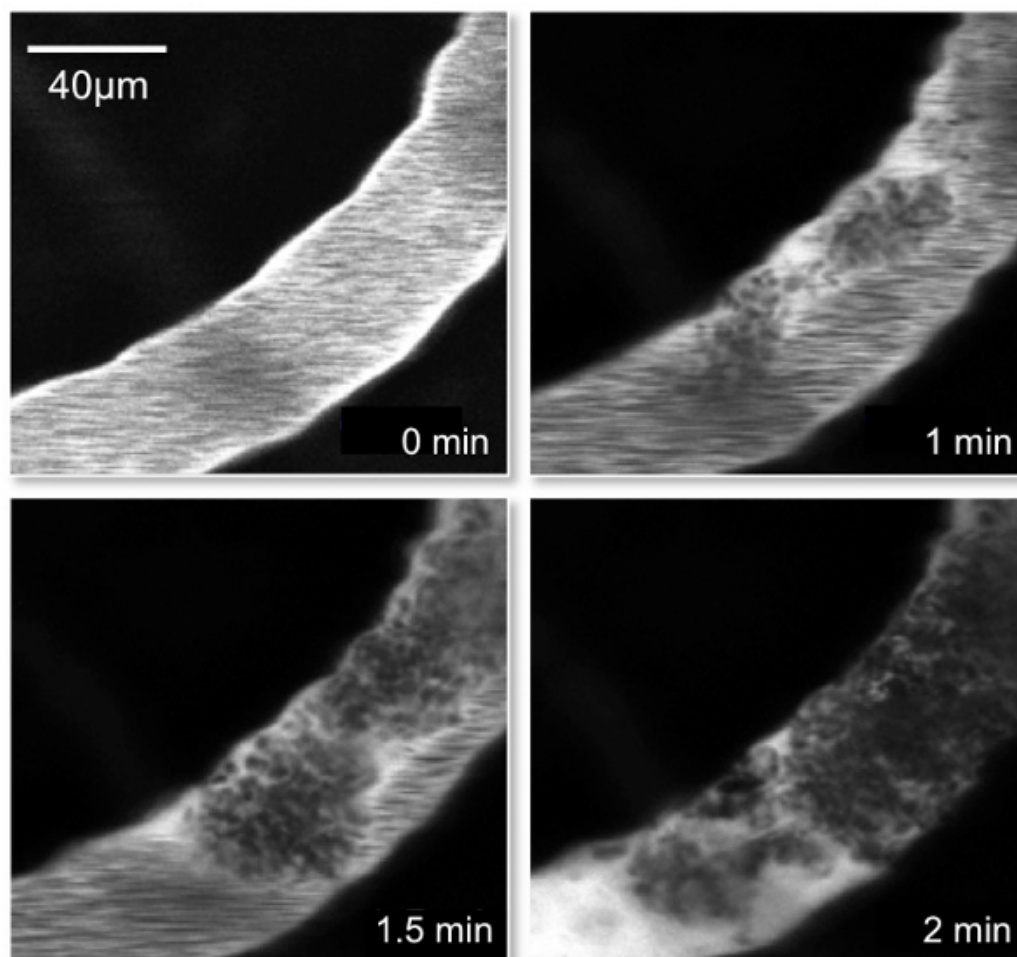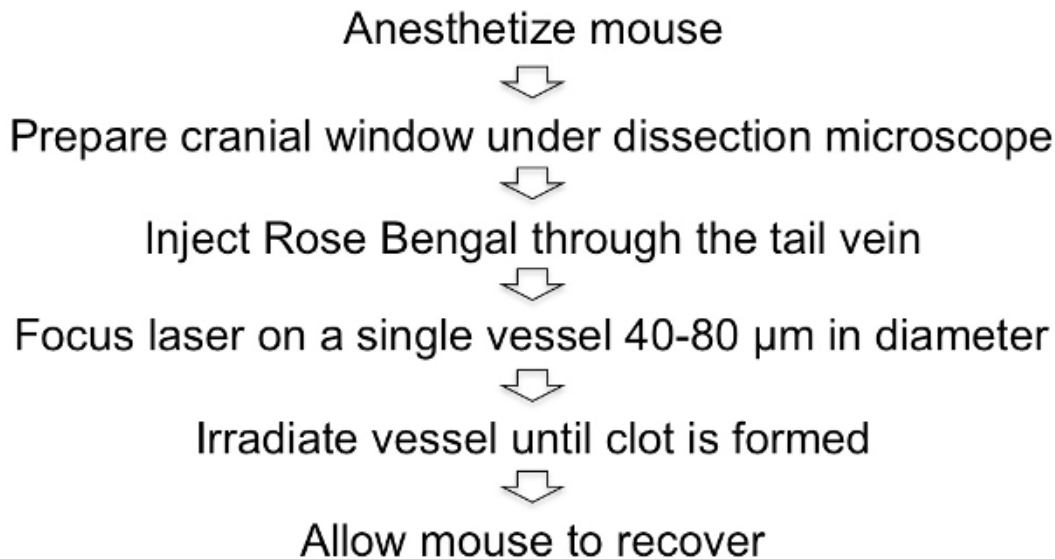
Figure 4: Picture of Rose Bengal Clot formation. Representative images of a single vessel containing Rose Bengal dye that was injected through the tail vein of the mouse. The images demonstrate the progression of clot formation within the vessel following irradiation of the area at 0, 1, 1.5 and 2 min. Note the accumulation of the Rose Bengal dye (white) preceding the clot (black) in the 2 min frame demonstrating the complete occlusion of the artery.
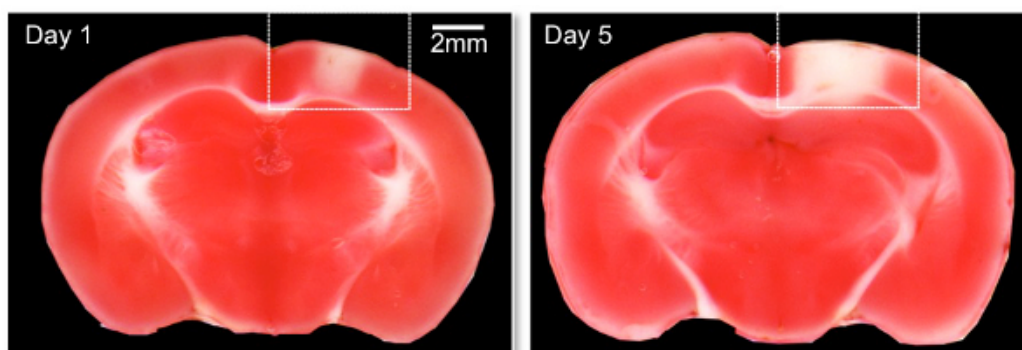
Figure 5: 2,3,5-triphenyltetrazolium chloride (TTC) image of RB induced lesion. Representative images are shown on Day 1 and 5 post-photothrombosis induction. The mice were sacrificed and the brains rapidly removed and sliced into 1mm coronal sections and stained with TTC according to standard methods. TTC is a commonly used stain for the detection of cerebral infarction by the formation of red formazan TTC products in healthy tissue. The lack of formazan production (white tissue) indicates the infarct area. The areas indicated by the boxes demonstrate the typical lesion sizes obtained following a clot produced within a vessel approximately 80 μm in diameter.

Anesthetize mouse

⇩

Prepare cranial window under dissection microscope

⇩

Inject Rose Bengal through the tail vein

⇩

Focus laser on a single vessel 40-80 μm in diameter

⇩

Irradiate vessel until clot is formed

⇩

Allow mouse to recover

Figure 6: Schematic representation of the Rose Bengal photothrombotic procedure.

Discussion

The ability to translate experimental stroke pathophysiology from animal to human application has been plagued with failure. However, the use of animal models, such as the photothrombosis model, allows for improved understanding of stroke pathophysiology and the exploration of new therapeutic approaches to provide neuroprotection following a stroke. Small cortical strokes and microinfarctions produced by the photothrombotic model are clinically relevant to subclinical or "silent" stroke[13-15], which has a high prevalence and affects approximately 4 percent of the United States population (about 11 million people) each year[16]. Silent stroke does not have the classic stroke symptoms present in a larger stroke, such as paralysis, sensory loss and difficulty speaking such as seen in the middle cerebral artery (MCA) occlusion or transient ischemic attack (TIA)[17]. Also, silent stroke is different from lacunar stroke, which is caused by occlusion of a single penetrating artery in deeper brain structures or within the brain stem and also clinically manifests with motor, sensory or mixed deficits[18]. Patients with subclinical or "silent" stroke typically do not display any outward symptoms and are often unaware they have even suffered a stroke. Silent stroke results in a subclinical decrease in cognitive function exhibited by deficits in memory, decision-making, and changes in behavior. Over time, multiple silent strokes lead to clinically significant signs of memory loss known as vascular or multi-infarct dementia. However, silent stroke brain damage can be detected using neuroimaging, and places a patient at risk for TIA and major stroke in the future[19].

The photothrombosis model allows for the production of a reproducible *in vivo* model of thrombosis in an intact, anesthetized mouse using the photosensitive dye Rose Bengal (RB) in combination with confocal microscopy. There are many advantages of the *in vivo* photothrombosis model. One advantage of this method is the ability to predefine the location of the stroke using stereotaxic coordinates; allowing one to study particular cell populations across animals. Additionally, the reproducibility of lesion size and volume is well controlled utilizing this method by varying the intensity of the laser light and controlling for vessel size being irradiated[20]. This method also allows for detailed study of changes in peri-infarct neurotransmission and corresponding contralateral cortex[4]. Though a single silent stroke causes minimal deficits, the reproducibility of this model allows for the ability to induce multiple silent strokes in specific areas, which can be used to mimic various brain dysfunctions such as vascular dementia. Development of a threshold between multiple silent strokes and clinically evident deficits could be determined in specific areas of the brain through the use of this method as well. Finally, the model allows for longitudinal studies in the same animal allowing for both acute and chronic effects to be observed.

There are, however, some disadvantages in using the photothrombosis model. One disadvantage includes the production of a lesion that is noted as having a small ischemic penumbra when compared to other models of focal stroke[4]. Secondly, vasogenic and cytotoxic edema formation is possible due to the damage that may occur during the induction of photothrombosis, which more closely resembles traumatic brain injuries than focal stroke[4].

When using the photothrombosis model there are a number of factors that must be monitored throughout the experiment. It is critical that the physiological state of the animal be monitored throughout all imaging procedures. It is well known that anesthesia level can affect the physiological status of the animal, with over anesthetizing causing decreased heart rate and oxygen delivery to the animal. This is an important consideration, as this would decrease the availability of oxygen to the brain resulting in global ischemia. Therefore, the use of a system to monitor the physiological status of the animal will allow for the simultaneous non-invasive recording of:Arterial Oxygen Saturation (SpO$_2$); Heart Rate; Breath Rate; Pulse Distention (indicator of local blood flow and signal quality); Breath Distention (surrogate for intraplueral pressure); and core temperature in mice and rats. It is becoming increasingly important to control for anesthesia confounds when working with any animal model to reduce unexpected confounds in translating experimental results to benefits in clinical stoke. The choice, duration and depth of anesthesia can have a drastic impact in animal model of experimental stroke. Studies have demonstrated that anesthetic agents may reduce infarct size and may even provide some protection from cerebral ischemia[21-23,24]. Additionally, alterations in the production of reactive oxygen species has also been demonstrated in a study comparing the use of halothane and propofol[25]. This confound is important as one of the primary hypotheses in neuronal death associated with stroke is the production of reactive oxygen species.

One complication of utilizing *in vivo* microscopy to study the response of the brain to a stroke is the limitation of the imaging depth achievable. In our laboratory using confocal microscopy the imaging depth that can be achieved is in the range of 100-200 μm, while using a two-photon

microscope can increase this depth to between 400-500 µm. These confounds are being alleviated by the development of objectives with increased working distances and of decreasing size. For example, the gradient refractive index (GRIN) microlenses are microendoscopes with diameters between 35-1,000 µm and are the smallest available to date. This type of probe cannot be inserted into the tissue without causing invasive damage and have low numerical apertures. Due to the low NA the resolution is inferior compared to traditional optical microscopy objectives[26].

In summary, the Rose Bengal photothrombosis model induces an infarct of small size and is useful in studying the cellular response to an infarct in both the acute and chronic phases in a well defined cellular population. This model demonstrates essential cellular characteristics seen with focal ischemia following MCAO and therefore is useful in assessing neuroprotective/neuroregenerative therapies.

Disclosures

The authors declare that they have no competing financial interests.

Acknowledgements

References

1. Watson, B. D., Dietrich, W. D., Busto, R., Wachtel, M. S., Ginsberg, M. D. Induction of reproducible brain infarction by photochemically initiated thrombosis. *Annals of Neurology.* **17**, 497-504 (1985).
2. Rosenblum, W. I., El-Sabban, F. Platelet aggregation in the cerebral microcirculation: effect of aspirin and other agents. *Circulation Research.* **40**, 320-328 (1977).
3. Owens, A. P. 3rd, Mackman, N. Sources of tissue factor that contribute to thrombosis after rupture of an atherosclerotic plaque. *Thrombosis Research.* **129**, Suppl 2. S30-S33 (2012).
4. Carmichael, S. T. Rodent models of focal stroke: size, mechanism, and purpose. *NeuroRx : the journal of the American Society for Experimental NeuroTherapeutics.* **2**, 396-409 (2005).
5. *Manual of stroke models in rats.* 332 CRC Press (2009).
6. Herz, R. C., Kasbergen, C. M., Hillen, B., Versteeg, D. H., de Wildt, D. J. Rat middle cerebral artery occlusion by an intraluminal thread compromises collateral blood flow. *Brain Research.* **791**, 223-228 (1998).
7. Brint, S., Jacewicz, M., Kiessling, M., Tanabe, J., Pulsinelli, W. Focal brain ischemia in the rat: methods for reproducible neocortical infarction using tandem occlusion of the distal middle cerebral and ipsilateral common carotid arteries. *Journal of Cerebral Blood Flow and Metabolism : Official Journal of the International Society of Cerebral Blood Flow and Metabolism.* **8**, 474-485 (1988).
8. Zheng, W., *et al.* Purinergic receptor stimulation reduces cytotoxic edema and brain infarcts in mouse induced by photothrombosis by energizing glial mitochondria. *PloS One.* **5**, e14401 (2010).
9. Zheng, D. M., Wewer, J., Lechleiter, J. P. 2Y. 1R. -initiated IP3R-dependent stimulation of astrocyte mitochondrial metabolism reduces and partially reverses ischemic neuronal damage in mouse. *Journal of Cerebral Blood Flow and Metabolism.* **33**, 600-611 (2013).
10. Witte, O. W., Stoll, G. Delayed and remote effects of focal cortical infarctions: secondary damage and reactive plasticity. *Advances in Neurology.* **73**, 207-227 (1997).
11. Hagemann, G., Redecker, C., Neumann-Haefelin, T., Freund, H. J., Witte, O. W. Increased long-term potentiation in the surround of experimentally induced focal cortical infarction. *Annals of Neurology.* **44**, 255-258 (1998).
12. Kramer, M., *et al.* TTC staining of damaged brain areas after MCA occlusion in the rat does not constrict quantitative gene and protein analyses. *Journal of Neuroscience Methods.* **187**, 84-89 (2010).
13. Blinder, P., Shih, A. Y., Rafie, C., Kleinfeld, D. Topological basis for the robust distribution of blood to rodent neocortex. *Proceedings of the National Academy of Sciences.* **107**, 12670-12675 (2010).
14. Nishimura, N., Rosidi, N. L., Iadecola, C., Schaffer, C. B. Limitations of collateral flow after occlusion of a single cortical penetrating arteriole. *Journal of Cerebral Blood Flow & Metabolism.* **30**, 1914-1927 (2010).
15. Nishimura, N., Schaffer, C. B., Friedman, B., Lyden, P. D., Kleinfeld, D. Penetrating arterioles are a bottleneck in the perfusion of neocortex. *Proceedings of the National Academy of Sciences.* **104**, 365 (2007).
16. Blum, S., *et al.* Memory after silent stroke: Hippocampus and infarcts both matter. *Neurology.* **78**, 38-46 (2012).
17. Heinsius, T., Bogousslavsky, J., Van Melle, G. Large infarcts in the middle cerebral artery territory Etiology and outcome patterns. *Neurology.* **50**, 341-350 (1998).
18. Wardlaw, J. What causes lacunar stroke. *Journal of Neurology, Neurosurgery & Psychiatry.* **76**, 617-619 (2005).
19. Inoue, Y., *et al.* Ischemic stroke under anticoagulant therapy]. Rinsho shinkeigaku. *Clinical Neurology.* **50**, 455-460 (2010).
20. Tiannan Wang, W. C., Xie, Y., Zhang, W., Ding, S. Controlling the Volume of the Focal Cerebral Ischemic Lesion through Photothrombosis. *American Journal of Biomedical Sciences.* **2**, 33-42 (2009).
21. Head, B. P., Patel, P. Anesthetics and brain protection. *Current Opinion in Anaesthesiology.* **20**, 395-399 (2007).
22. Kirsch, J. R., Traystman, R. J., Hurn, P. D. Anesthetics and cerebroprotection: experimental aspects. *International Anesthesiology Clinics.* **34**, 73-93 (1996).
23. Koerner, I. P., Brambrink, A. M. Brain protection by anesthetic agents. *Current Opinion in Anaesthesiology.* **19**, 481-486 (2006).
24. Gelb, A. W., Bayona, N. A., Wilson, J. X., Cechetto, D. F. Propofol anesthesia compared to awake reduces infarct size in rats. *Anesthesiology.* **96**, 1183-1190 (2002).

25. Bhardwaj, A., Castro, I. A., Alkayed, N. J., Hurn, P. D., Kirsch, J. R. Anesthetic choice of halothane versus propofol: impact on experimental perioperative stroke. *Stroke; A Journal Of Cerebral Circulation.* **32**, 1920-1925 (2001).

26. Barretto, R. P., Messerschmidt, B., Schnitzer, M. J. In vivo fluorescence imaging with high-resolution microlenses. *Nature Methods.* **6**, 511-512 (2009).